RSC Advances

COMMUNICATION

View Article Online
View Journal | View Issue

Cite this: *RSC Adv.*, 2014, **4**, 21553

Received 12th March 2014
Accepted 29th April 2014

DOI: 10.1039/c4ra02168a

www.rsc.org/advances

Ultra-light nanocomposite aerogels of bacterial cellulose and reduced graphene oxide for specific absorption and separation of organic liquids†

Yonggui Wang,‡[a] Sandeep Yadav,‡[b] Thorsten Heinlein,[b] Valentino Konjik,[a] Hergen Breitzke,[c] Gerd Buntkowsky,[c] Jörg J. Schneider*[b] and Kai Zhang*[a]

Novel materials based on sustainable materials with high absorption capacity are still rare for the separation of organic liquids or oil spills and water. In this report, ultra-light nanocomposite aerogels consisting of sustainable bacterial cellulose (BC) and graphene oxide (GO) were constructed after an eco-friendly freeze-drying process for the first time. Due to the hydrophilic properties of both materials and the highly porous structure, BC/GO aerogels could highly absorb not only organic liquids, such as cyclohexane and DMF, but also water. Specific absorption for organic liquids was achieved after the reduction of GO using H_2 gas, which led to nanocomposite aerogels of BC and reduced GO. They could specifically absorb 135–150 g organic liquids per g of their own weight, even with a high content of 80% BC in the nanocomposite aerogel.

Separating water and oil spills or organic liquids has become more relevant in recent years due to many facts including environmental, health, and economic issues, *e.g.* wastewater from industries, and oil spills from oil tankers or ship accidents. In particular, it is of particular interest to separate organic pollutants and water, such as hydrogen and carbon based solvents.[1,2] In the last few years, a couple of porous materials in the form of aerogel and foam have been used for the separation of organic solvents and water.[3] Polypropylene fiber mats,[4] polyurethane sponges coated with block copolymer consisting of poly(2-vinylpyridine) and polydimethylsiloxane,[5] as well as inorganic absorbents including clay[6] and manganese oxide nanoweb[2] suffer from low absorption capacity of up to 50 times of original weights. Ultralight silicon aerogels have also been used as absorbents for organic oils and spills, but they suffer from the brittleness and low absorption capacity.[7] Among most used absorbents for organic oils and spills, carbon nanotube (CNT) aerogels,[8] graphene,[9] CNT/graphene composite,[10] polyurethane sponges coated with reduced graphene oxide[11] and carbon nanofiber aerogels[12,13] showed high absorption capacity of 80–950 times of their own weights. Very recently, novel progresses were made to fabricate functional absorbents for organic solvents. Polyurethane foam containing magnetite, core–shell Fe_2O_3@C nanoparticles or pH-responsive copolymers were used because they can be simply removed after the absorption of organic contaminants.[5,14,15] Various conventional methods have been widely used, which include separation *via* ultrasonication, gravity, centrifugation, membrane filtration and biological treatments.[3] Due to the limitations such as slow separation, low separation efficiency and/or selectivity, recycling problems of used absorbents and even pollutants released during the preparation of absorbents, the demand on novel, efficient and green materials encourage the research on developing new materials for separating organic pollutants and water.

In comparison to the aforementioned materials, sustainable, naturally occurring green materials, *e.g.* cellulose, have been less used for the separation of oily compounds.[16,17] In these studies, the surface of cellulose fibers has to be hydrophobized *via* deposition of silanes or titanium dioxide, in order to suppress the strong interaction between native cellulose and water. Moreover, cellulose aerogels with increased volume were used for the separation of oily compounds due to their porous structure.[16,17] By introducing another component into cellulose aerogel, resulted nanocomposite aerogels with novel functions can be obtained. For instance, cellulose-based nanocomposite aerogels containing graphene oxide (GO) have also been reported very recently for the fabrication of superhydrophobic surface and flexible supercapacitors.[18,19] However, due to strong interaction of GO with water, these aerogels containing

[a]*Ernst-Berl-Institute for Chemical Engineering and Macromolecular Science, Technische Universität Darmstadt, Alarich-Weiss-Straße 8, D-64287 Darmstadt, Germany. E-mail: zhang@cellulose.tu-darmstadt.de*

[b]*Inorganic Chemistry, Eduard-Zintl-Institute for Inorganic Chemistry and Physical Chemistry, Technische Universität Darmstadt, Alarich-Weiss-Straße 12, D-64287 Darmstadt, Germany. E-mail: joerg.schneider@ac.chemie.tu-darmstadt.de*

[c]*Physical Chemistry, Eduard-Zintl-Institute for Inorganic Chemistry and Physical Chemistry, Technische Universität Darmstadt, Alarich-Weiss-Straße 4, D-64287 Darmstadt, Germany*

† Electronic supplementary information (ESI) available. See DOI: 10.1039/c4ra02168a

‡ These authors contributed equally to this work.

cellulose and GO cannot be used for the specific separation of oily compounds. Cellulose aerogels can be prepared using various plant celluloses, nanocrystalline cellulose or bacterial cellulose.[20–24] Bacterial cellulose (BC) attracts more attention in last years, since it exhibits high purity, high crystallinity and high aspect ratio.[25] Its single fibrils showed average diameter lower than 100 nm, while the length can be >100 μm.[25,26] Crystalline cellulose has exhibited excellent mechanical properties, which are comparable to many other reinforcement materials including carbon nanotubes and steel.[27] In this report, an efficient method for the fabrication of novel nanocomposite aerogel based on sustainable bacterial cellulose (BC) and graphene oxide (GO) was reported for the construction of superabsorbent for organic liquids. Ultra-light aerogels of BC and nanocomposite BC/GO were constructed after eco-friendly freeze-drying process, which showed high absorption capacity not only to organic liquids but also water. BC/GO aerogels underwent further reduction in H_2 flow leading to BC/rGO nanocomposite aerogels, which exhibited specific absorption only for organic liquids.

Bacterial cellulose (BC) in aqueous suspension was fibrillated and then freeze-dried leading to aerogel (Fig. 1a). BC has a highly crystalline structure with a crystallinity of 84% according to solid-state ^{13}C NMR spectroscopy (Fig. 1b).[28,29] It is well known that crystalline cellulose exhibited excellent mechanical properties, which are comparable to many other reinforcement materials including carbon nanotubes and steel.[27] Furthermore, BC fibrils have diameters averagely lower than 100 nm.[30] These advantages allows BC to be excellent structure materials in various (nano)composites.[31,32] By incorporating graphene oxide (GO) (Fig. S1†)[33] in the BC suspension, ultra-light aerogels were also obtained after freeze-drying. Their forms did not changed after the subsequent reduction of GO at 200 °C for 4 h (Fig. 1a). The reduction of GO is reflected by the presence of new bands at 1573, 1000 and 984 cm^{-1} as well as the disappearance of the signal at 1632 cm^{-1} in their FTIR spectra (Fig. 1c). Thus, the carboxyl groups should have been almost totally reduced, while the ketones still maintained according to the signal at 1724 cm^{-1}. The reduction time of BC/GO nanocomposites was set at 4 h according to the FTIR spectroscopic analysis (Fig. S2†). At the same time, BC did not undergo any significant modification at 200 °C under H_2 flow for 4 h (Fig. 1c).

All aerogels prepared in the present study are highly porous, as demonstrated *via* scanning electron microscopy (SEM) (Fig. 2a–e). The porosities of BC and BC/GO with two different ratios, 80/20 and 50/50, were determined to be 99.92 ± 0.02%, 99.84 ± 0.01% and 99.86 ± 0.01%, respectively. Moreover, the morphologies of cellulose fibers in BC aerogel and nanocomposite aerogels are slightly different. The BC fibrils in BC aerogel are present as individual flexible fibrils (Fig. 2a), which are bound together only *via* hydrogen bonds.[23,25,30] Within the nanocomposite aerogel of BC/GO (80/20), fewer single BC fibrils are visible (Fig. 2b), which is ascribed to the enhanced binding between BC fibrils by GO nanosheets. With increasing content of GO within the aerogels from 20% to 50%, almost only micro-sized sheets instead of individual BC fibrils are visible (Fig. 2c). Slightly morphological difference can be traced according to transmission electron microscope (TEM) images of BC, rGO and BC/rGO composites, where BC nanofibrils in the composites led to more rough surfaces compared to rGO nanosheet alone (Fig. 2f–i). Thus, BC nanofibrils and rGO nanosheets are intimately compounded together forming a dense and homogeneous composite with the morphology of planar ultrathin sheet. The reduction of nanocomposite aerogels did not significantly change the morphologies of these microscaled sheets (Fig. 2d and e).

Various porous nanocomposites aerogels using BC have been prepared previously, *e.g.* with synthetic polymers, carbon nanotubes and recently with GO.[20,31,32,34,35] BC/GO aerogels have been used for the fabrication of superhydrophobic surface after further surface deposition of perfluorinated silanes or flexible supercapacitors.[18,19] However, nanocomposite aerogels based on these sustainable materials have not been used for the separation of organic liquids and water. For this purpose, the absorption capacity of cellulose-based nanocomposite aerogels towards organic liquids was examined at first (Fig. 3a and b). Dimethylformamide (DMF) and cyclohexane were representatively chosen because (1) they are very commonly used in many different fields; and (2) they represent polar, protic, water-miscible and non-polar, aprotic, water non-miscible organic solvent, respectively.

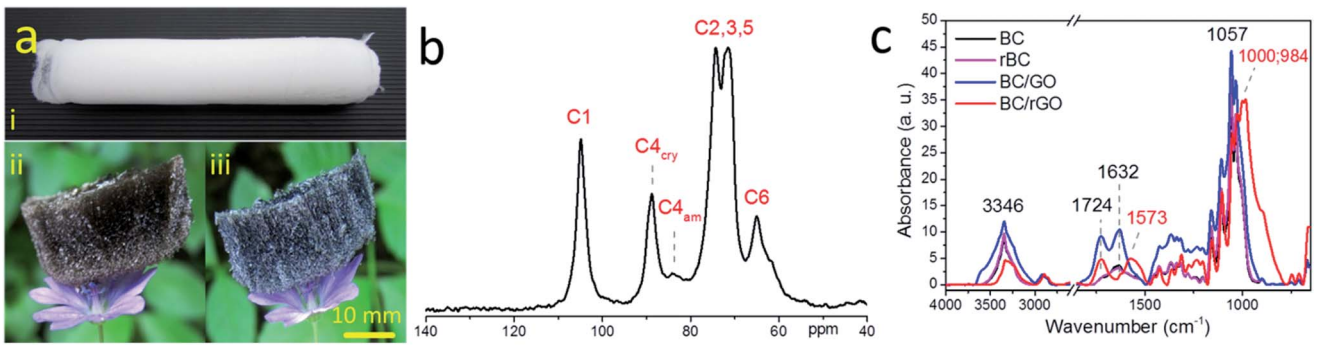

Fig. 1 (a) Photo images of aerogels from (i) BC; (ii) BC/GO (50/50) hold by a flower and (iii) BC/rGO (50/50) after the reduction hold by a flower. Scale bar: 10 mm. (b) Solid-state ^{13}C NMR spectrum of BC. (c) FTIR spectra of aerogels from BC, rBC (BC treated under H_2 gas at 200 °C for 4 h), BC/GO and BC/rGO (BC/GO treated under H_2 gas at 200 °C for 4 h).

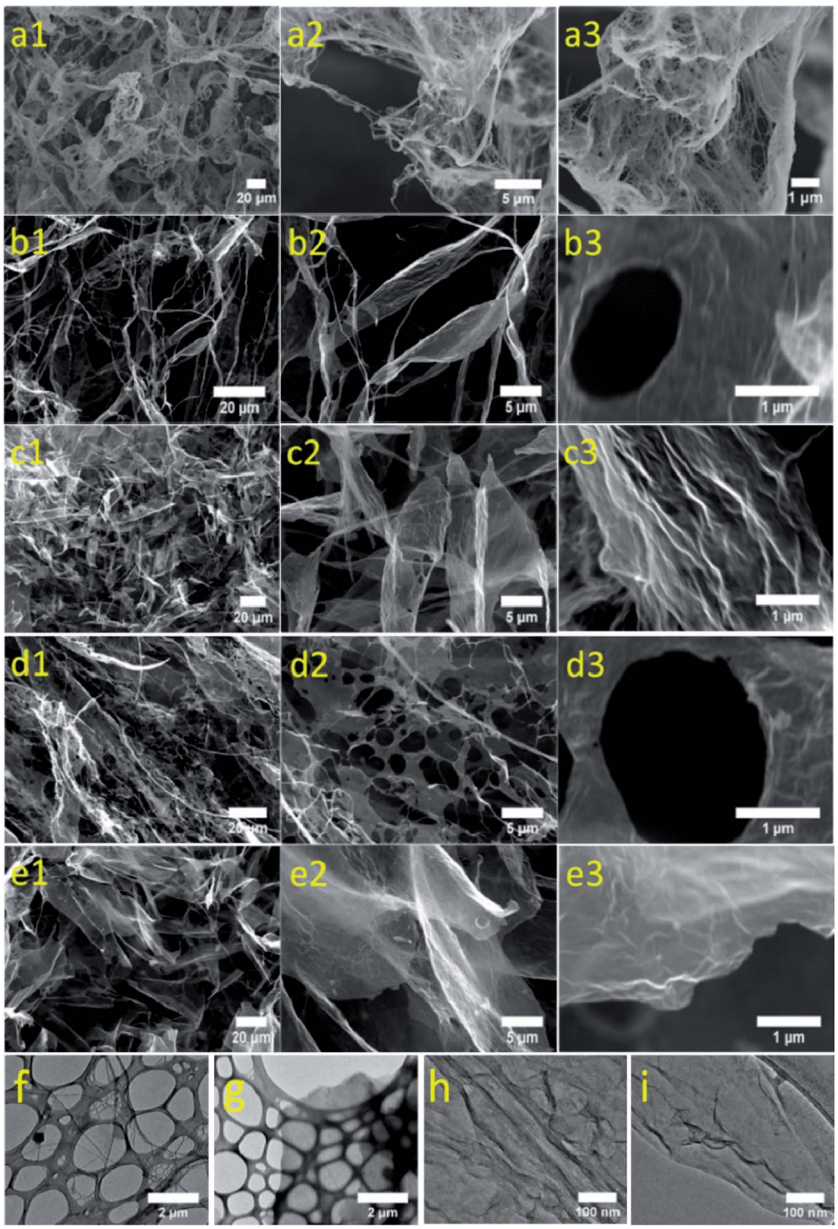

Fig. 2 (a–e) SEM images of (a) BC aerogel, (b) BC/GO aerogel (80/20), (c) BC/GO aerogel (50/50), (d) BC/rGO aerogel (80/20) and (e) BC/rGO aerogel (50/50) in three different magnifications. Scale bar in column 1: 20 μm, in column 2: 5 μm, and in column 3: 1 μm. (f–i) TEM images of (f) BC, (g) reduced GO, (h) BC/rGO aerogel (80/20), and (i) BC/rGO aerogel (50/50). Scale bar in (f) and (g) 2 μm; in (h) and (i) 100 nm.

As shown with these two organic solvents, aerogels of BC, BC/GO and BC/rGO all exhibited high absorption capacity of up to 147 g DMF and 164 g cyclohexane per g own weight, respectively (Fig. 3c). In comparison, although bare GO in water after a freeze-drying process formed aerogel, GO aerogel could not hold together after being put in organic solvents (Fig. S3†). BC aerogels and all composite aerogels could absorb cyclohexane more than DMF. BC aerogel could even absorb up to 164 g per g own weight, which is probably because of the amphiphilic character of crystalline cellulose.[36] With GO within the nanocomposite aerogel, the absorption capacities for both organic solvents were strongly reduced to <87 g DMF and <130 g cyclohexane per g own weight, respectively. The reduction extent increased with higher content of GO within the aerogel from 20% to 50% (Fig. 3c). This reduced capacity is probably because of enhanced hydrophilicity due to the presence of hydrophilic GO that contains carboxyl groups. In fact, after the reduction of GO, the absorption capacities for both organic liquids increased significantly to >136 g DMF and >150 g cyclohexane per g own weight correspondingly.

Ultraporous nanocellulose aerogels after the hydrophobization with silanes or coating with titanium dioxide demonstrated absorption capability for organic liquids, but they still suffered from the low absorption capacity of up to 50 times of own weight.[16,17,37] Hence, BC aerogel as well as BC/rGO

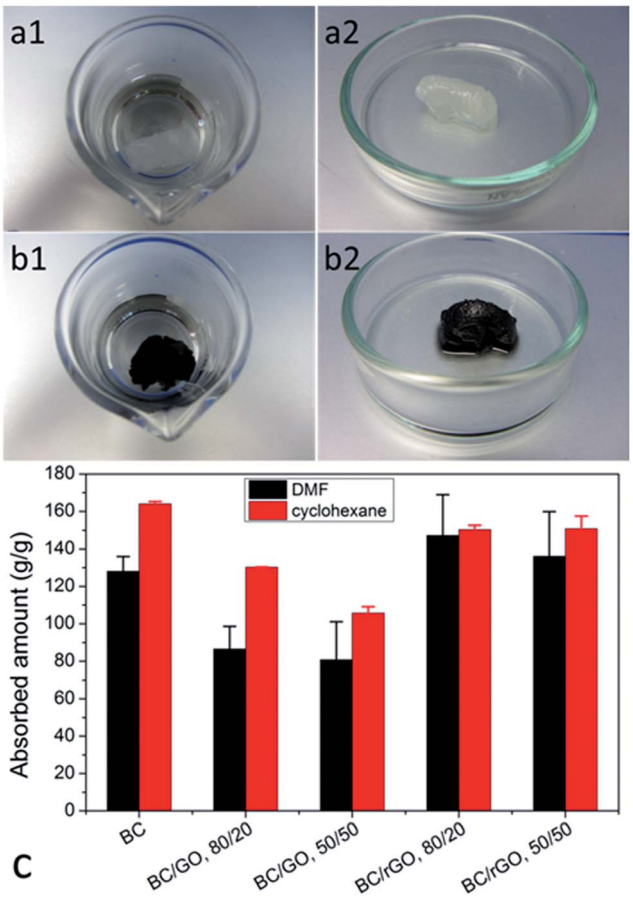

Fig. 3 Representative photo images for absorption experiment using (a) BC aerogel (b) BC/rGO (80/20) aerogel with column 1: within cyclohexane and column 2: aerogels containing cyclohexane. (c) Absorbed amounts of organic liquids by BC, BC/GO and BC/rGO aerogels.

nanocomposite aerogels exhibited much higher absorption capacity than those of aerogels from plant cellulose.

Porous BC and BC/GO aerogels could absorb both water and organic liquids at the same time, if placed on an organic liquid–water mixture (Fig. S4 and Movie S1†). In comparison, BC/rGO aerogels could selectively absorb organic liquids from water surface. After being placed on a mixture of cyclohexane (dyed with Sudan I) and water, BC/rGO aerogels (both 80/20 and 50/50) only absorbed cyclohexane quickly and specifically, leaving clean water (Fig. S4†). After the absorption of either water or organic liquids, all aerogels generally shrunk up.

To intuitively demonstrate the specific absorption capacity of aerogels, another experiment was operated, where the organic liquids were added later. Based on the experiments, it is clear if BC and BC/GO aerogels have absorbed sufficient amount of water, they could not absorb subsequently added organic liquids any more (Fig. 4a, Movie S2 and S3†). In contrast, BC/rGO aerogels (both 80/20 and 50/50) did not uptake any water, while only subsequently added cyclohexane was rapidly absorbed (Fig. 4a, Movie S4†). Moreover, the content of rGO in the nanocomposite seemed not to affect the absorption capacity.

Because BC and BC/GO aerogels can strongly interact both with water and organic solvents at the same time, the absorption capacity of BC or BC/GO aerogels is primarily derived from the porous structure of aerogels. Due to the presence of individual amphiphilic nano-scaled BC fibrils, BC aerogels are more non-polar than BC/GO aerogels. In comparison, BC/rGO aerogels with identical porous structure as BC/GO aerogels could only specifically absorb organic solvents and thus exhibited increased non-polarity and oleophilicity than BC/GO aerogels. Because only BC fibrils are hydrophilic components in the composite aerogels after the reduction, the surface of BC fibrils

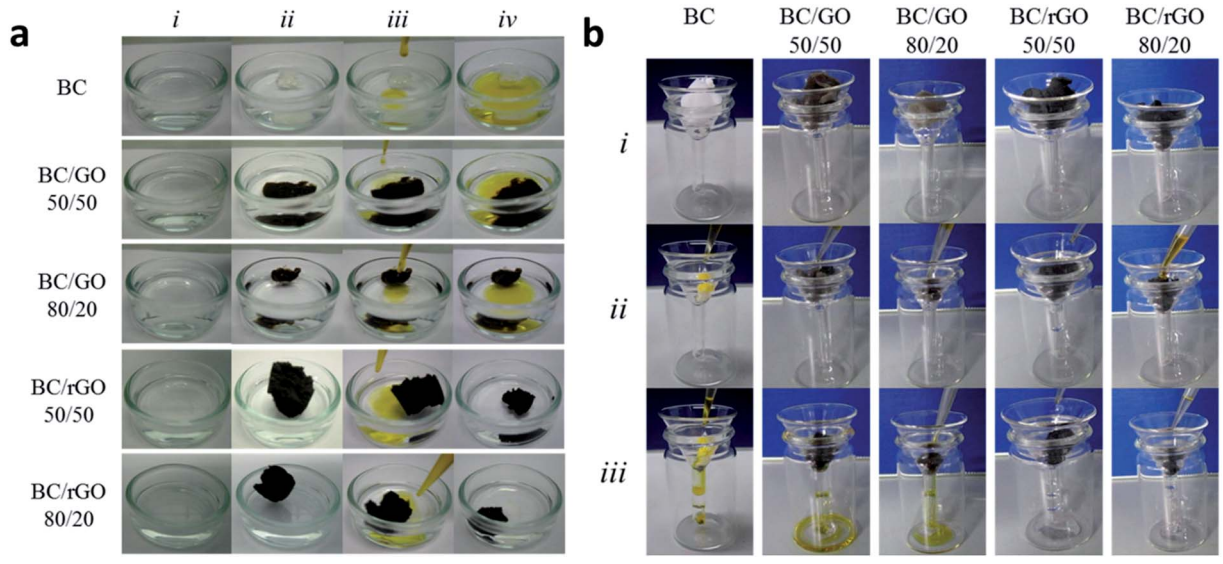

Fig. 4 (a) Representative snapshots showing the absorption of cyclohexane (dyed with Sudan I) from water surface with column (i) pure water in petri dishes; (ii) placement of aerogels onto water surface; (iii) begin of the addition of dyed cyclohexane; (iv) end of the addition of dyed cyclohexane. (b) Representative snapshots showing the separation of cyclohexane (dyed with Sudan I) and water from their mixture with row (i) placement of aerogels into funnels; (ii) begin of the addition of dyed cyclohexane–water mixture; (iii) end of the addition of dyed cyclohexane–water mixture.

should have been totally decorated or surrounded by rGO nanosheets (Fig. 2).

Simple separations directly *on line* are often desired in the practical applications, *e.g.* filtration of the liquid flow, so that no intermediate stop is necessary. Currently, such separation of organic liquids and water was generally realized with membranes.[2,38] It is further demonstrated with another designed experiment that the aerogels can be used for such *on line* separation. With aerogels on a small funnel, a mixture of cyclohexane (dyed with Sudan I) and water was added (Fig. S5†). Based on the porous structure and amphiphilicity of BC and BC/GO aerogels, they absorb simultaneously both water and organic liquids, until the aerogels reached maximal absorption capacity (Fig. 4b). Then, the excess water and cyclohexane flowed into the vessels together (Movie S5 and S6†). With strongly enhanced oleophilicity, BC/rGO aerogels exhibited specific absorption of cyclohexane in its mixture with water (Fig. 4b). Only water flowed through the edge of BC/rGO aerogel into the vessel after the addition of the mixture of cyclohexane and water (Fig. 4b, Movie S7†).

In summary, an efficient method for the preparation of novel aerogels based on sustainable bacterial cellulose (BC) and non-reduced or reduced graphene oxide (GO or rGO) was reported, which exhibited the superabsorbent property for organic liquids. The aerogels showed high absorption capacities for selected organic liquids, DMF and cyclohexane, of up to 147 g and 164 g per g own weight, respectively. With increasing GO within the nanocomposite aerogels (BC/GO at the ratio of 80/20 and 50/50), the absorption capacity for the organic liquids decreased. After the reduction of GO, obtained nanocomposite aerogel (BC/rGO) exhibited again specific absorption for the organic liquids. Thus, the amphiphilic property of BC nanofibrils should have been impacted by the decoration or surrounding with GO nanosheets. After the reduction, only hydrophobic property of reduced GO dominated. Obtained BC/rGO nanocomposite aerogels showed the feasibility to separate organic liquids from their mixtures with water *via* absorption or during liquid flow. The conversion of GO within an aerogel into reduced rGO represents a general, effective method for the construction of novel materials for the separation of organic liquids and water.

Acknowledgements

Financial support from LOEWE – Research Cluster "Soft Control" (KZ and AG) and from LOEWE – Research Cluster "Sensors towards Terahertz STT" (JJS and TH) is gratefully acknowledged. KZ thanks Prof. Markus Biesalski for the kind support. (The experimental section including the methods for the fabrication of aerogels and characterizations are included in ESI.†)

Notes and references

1 L. Feng, Z. Zhang, Z. Mai, Y. Ma, B. Liu, L. Jiang and D. Zhu, *Angew. Chem., Int. Ed.*, 2004, **43**, 2012–2014.
2 J. Yuan, X. Liu, O. Akbulut, J. Hu, S. L. Suib, J. Kong and F. Stellacci, *Nat. Nanotechnol.*, 2008, **3**, 332–336.
3 Z. Xue, Y. Cao, N. Liu, L. Feng and L. Jiang, *J. Mater. Chem. A*, 2014, **2**, 2445–2460.
4 S. J. Choi, T. H. Kwon, H. Im, D. I. Moon, D. J. Baek, M. L. Seol, J. P. Duarte and Y. K. Choi, *ACS Appl. Mater. Interfaces*, 2011, **3**, 4552–4556.
5 L. Zhang, Z. Zhang and P. Wang, *NPG Asia Mater.*, 2012, **4**, e8.
6 O. Carmody, R. Frost, Y. Xi and S. Kokot, *J. Colloid Interface Sci.*, 2007, **305**, 17–24.
7 A. Venkateswara Rao, N. D. Hegde and H. Hirashima, *J. Colloid Interface Sci.*, 2007, **305**, 124–132.
8 X. Gui, J. Wei, K. Wang, A. Cao, H. Zhu, Y. Jia, Q. Shu and D. Wu, *Adv. Mater.*, 2010, **22**, 617–621.
9 Y. Zhao, C. Hu, Y. Hu, H. Cheng, G. Shi and L. Qu, *Angew. Chem., Int. Ed.*, 2012, **51**, 11371–11375.
10 H. Sun, Z. Xu and C. Gao, *Adv. Mater.*, 2013, **25**, 2554–2560.
11 Y. Liu, J. Ma, T. Wu, X. Wang, G. Huang, H. Qiu, Y. Li, W. Wang and J. Gao, *ACS Appl. Mater. Interfaces*, 2013, **5**, 10018–10026.
12 H. Bi, Z. Yin, X. Cao, X. Xie, C. Tan, X. Huang, B. Chen, F. Chen, Q. Yang, X. Bu, X. Lu, L. Sun and H. Zhang, *Adv. Mater.*, 2013, **25**, 5916–5921.
13 Z. Y. Wu, C. Li, H. W. Liang, J. F. Chen and S. H. Yu, *Angew. Chem., Int. Ed.*, 2013, **52**, 2925–2929.
14 P. Calcagnile, D. Fragouli, I. S. Bayer, G. C. Anyfantis, L. Martiradonna, P. D. Cozzoli, R. Cingolani and A. Athanassiou, *ACS Nano*, 2012, **6**, 5413–5419.
15 Q. Zhu, F. Tao and Q. Pan, *ACS Appl. Mater. Interfaces*, 2010, **2**, 3141–3146.
16 N. T. Cervin, C. Aulin, P. T. Larsson and L. Wågberg, *Cellulose*, 2011, **19**, 401–410.
17 J. T. Korhonen, M. Kettunen, R. H. Ras and O. Ikkala, *ACS Appl. Mater. Interfaces*, 2011, **3**, 1813–1816.
18 K. Gao, Z. Shao, J. Li, X. Wang, X. Peng, W. Wang and F. Wang, *J. Mater. Chem. A*, 2013, **1**, 63.
19 A. Javadi, Q. Zheng, F. Payen, Y. Altin, Z. Cai, R. Sabo and S. Gong, *ACS Appl. Mater. Interfaces*, 2013, **5**, 5969–5975.
20 J. Cai, S. Liu, J. Feng, S. Kimura, M. Wada, S. Kuga and L. Zhang, *Angew. Chem., Int. Ed.*, 2012, **51**, 2076–2079.
21 J. Innerlohinger, H. K. Weber and G. Kraft, *Macromol. Symp.*, 2006, **244**, 126–135.
22 F. Liebner, E. Haimer, M. Wendland, M. A. Neouze, K. Schlufter, P. Miethe, T. Heinze, A. Potthast and T. Rosenau, *Macromol. Biosci.*, 2010, **10**, 349–352.
23 R. T. Olsson, M. A. S. A. Samir, G. Salazar-Alvarez, L. Belova, V. Strom, L. A. Berglund, O. Ikkala, J. Nogues and U. W. Gedde, *Nat. Nanotechnol.*, 2010, **5**, 584–588.
24 C. B. Tan, B. M. Fung, J. K. Newman and C. Vu, *Adv. Mater.*, 2001, **13**, 644–646.
25 D. Klemm, D. Schumann, U. Udhardt and S. Marsch, *Prog. Polym. Sci.*, 2001, **26**, 1561–1603.
26 C. H. Haigler, A. R. White, R. M. Brown, Jr and K. M. Cooper, *J. Cell Biol.*, 1982, **94**, 64–69.
27 R. J. Moon, A. Martini, J. Nairn, J. Simonsen and J. Youngblood, *Chem. Soc. Rev.*, 2011, **40**, 3941–3994.

28 P. T. Larsson, K. Wickholm and T. Iversen, *Carbohydr. Res.*, 1997, **302**, 19–25.
29 P. T. Larsson, E. L. Hult, K. Wickholm, E. Pettersson and T. Iversen, *Solid State Nucl. Magn. Reson.*, 1999, **15**, 31–40.
30 K. Zhang, *Appl. Microbiol. Biotechnol.*, 2013, **97**, 4353–4359.
31 E. E. Brown and M. P. Laborie, *Biomacromolecules*, 2007, **8**, 3074–3081.
32 A. Nakayama, A. Kakugo, J. P. Gong, Y. Osada, M. Takai, T. Erata and S. Kawano, *Adv. Funct. Mater.*, 2004, **14**, 1124–1128.
33 D. C. Marcano, D. V. Kosynkin, J. M. Berlin, A. Sinitskii, Z. Sun, A. Slesarev, L. B. Alemany, W. Lu and J. M. Tour, *ACS Nano*, 2010, **4**, 4806–4814.
34 M. Hamedi, E. Karabulut, A. Marais, A. Herland, G. Nyström and L. Wågberg, *Angew. Chem., Int. Ed.*, 2013, **52**, 12038–12042.
35 M. Wang, I. V. Anoshkin, A. G. Nasibulin, J. T. Korhonen, J. Seitsonen, J. Pere, E. I. Kauppinen, R. H. Ras and O. Ikkala, *Adv. Mater.*, 2013, **25**, 2428–2432.
36 W. G. Glasser, R. H. Atalla, J. Blackwell, R. Malcolm Brown, W. Burchard, A. D. French, D. O. Klemm and Y. Nishiyama, *Cellulose*, 2012, **19**, 589–598.
37 M. Kettunen, R. J. Silvennoinen, N. Houbenov, A. Nykänen, J. Ruokolainen, J. Sainio, V. Pore, M. Kemell, M. Ankerfors, T. Lindström, M. Ritala, R. H. A. Ras and O. Ikkala, *Adv. Funct. Mater.*, 2011, **21**, 510–517.
38 G. Kwon, A. K. Kota, Y. Li, A. Sohani, J. M. Mabry and A. Tuteja, *Adv. Mater.*, 2012, **24**, 3666–3671.